Check for updates

Induction of photosynthesis under anoxic condition in *Thalassiosira pseudonana* and *Euglena gracilis*: interactions between fermentation and photosynthesis

Gwenaëlle Gain[1†‡], Nicolas Berne[1‡], Tom Feller[1],
Damien Godaux[1], Ugo Cenci[2] and Pierre Cardol[1*]

[1]InBioS − PhytoSYSTEMS, Laboratoire de Génétique et Physiologie des Microalgues, ULiège,
Liège, Belgium, [2]Unité de Glycobiologie Structurale et Fonctionnelle, Université de Lille, CNRS,
UMR8576 − UGSF, Lille, France

Introduction: In their natural environment, microalgae can be transiently exposed to hypoxic or anoxic environments. Whereas fermentative pathways and their interactions with photosynthesis are relatively well characterized in the green alga model *Chlamydomonas reinhardtii*, little information is available in other groups of photosynthetic micro-eukaryotes. In *C. reinhardtii* cyclic electron flow (CEF) around photosystem (PS) I, and light-dependent oxygen-sensitive hydrogenase activity both contribute to restoring photosynthetic linear electron flow (LEF) in anoxic conditions.

Methods: Here we analyzed photosynthetic electron transfer after incubation in dark anoxic conditions (up to 24 h) in two secondary microalgae: the marine diatom *Thalassiosira pseudonana* and the excavate *Euglena gracilis*.

Results: Both species showed sustained abilities to prevent over-reduction of photosynthetic electron carriers and to restore LEF. A high and transient CEF around PSI was also observed specifically in anoxic conditions at light onset in both species. In contrast, at variance with *C. reinhardtii*, no sustained hydrogenase activity was detected in anoxic conditions in both species.

Discussion: Altogether our results suggest that another fermentative pathway might contribute, along with CEF around PSI, to restore photosynthetic activity in anoxic conditions in *E. gracilis* and *T. pseudonana*. We discuss the possible implication of the dissimilatory nitrate reduction to ammonium (DNRA) in *T. pseudonana* and the wax ester fermentation in *E. gracilis*.

KEYWORDS

Euglena gracilis, *Thalassiosira pseudonana*, fermentation, photosynthesis, hydrogenase, cyclic electron flow (CEF)

1 Introduction

Some microalgae must cope with long or frequent hypoxic (low oxygen) or anoxic (no oxygen) events in many natural environments such as marine sediments, eutrophic standing shallow waters or ice (Drew, 1997; Banti et al., 2013; Catalanotti et al., 2013). This implies that these organisms are endowed with metabolic capacities such as fermentative pathways and associated electron acceptors which ensure the maintenance of the energy balance (ATP, NAD(P)H) in the dark, and in the light to restore photosynthetic activity. The green unicellular alga *Chlamydomonas reinhardtii* is the microalgal species whose fermentative pathways have been best characterized (Catalanotti et al., 2013). In anoxic conditions, *C. reinhardtii* synthesizes formate, acetate and ethanol as major terminal products (Kreuzberg, 1984; Mus et al., 2007) and some minor products such as hydrogen, lactate, glycerol and carbon dioxide (Atteia et al., 2013; Catalanotti et al., 2013). Three enzymes allow pyruvate conversion into acetyl-CoA: (i) the pyruvate dehydrogenase complex in aerobic conditions and (ii) the pyruvate formate lyase (PFL) and the pyruvate ferredoxin oxidoreductase (PFO) in anaerobiosis (Catalanotti et al., 2013). In the chloroplast, PFO generates acetyl-CoA and CO_2 by oxidative decarboxylation of pyruvate and generates reduced ferredoxin (FDX), which can be reoxidized by hydrogenases (HYDA1 and HYDA2), that catalyze proton reduction into H_2 (Catalanotti et al., 2013). Under anoxic conditions the excess of reduced equivalents may also affect photosynthetic linear electron flow (LEF) by increasing the redox state of pools of electron carriers and electron acceptors such as plastoquinones (PQ), FDX and NADPH. In *C. reinhardtii*, this is reflected by a marked decrease of variable chlorophyll (chl) fluorescence under anoxic conditions (Ghysels et al., 2013; Godaux et al., 2013; Clowez et al., 2015). In addition, a low ATP/NADPH ratio in the chloroplast impairs the activity of Calvin-Benson-Basham cycle (CBB) and therefore limits LEF from water to NADPH. In *C. reinhardtii*, two alternative photosynthetic electron flows (AEFs) contribute to restoring the balance of the ATP/NADPH ratio in the chloroplast upon illumination after acclimation to dark-anoxic conditions: the oxygen-sensitive HYDA1 hydrogenase that reoxidizes FDX reduced by photosystem (PS) I (Hemschemeier and Happe, 2011) and the cyclic electron flow (CEF) around PSI which recycles electrons from PSI acceptor side to intersystem electron carriers (PQ or cytochrome b_6f complex) (Clowez et al., 2015; Godaux et al., 2015). In *C. reinhardtii*, the absence of hydrogenase maturation factors (HYDG or HYDEF) impairs electron transfer during the first seconds of illumination under anoxic conditions (Ghysels et al., 2013; Godaux et al., 2013). In green plants, PGR5 and PGRL1 are the two main proteins that participate in CEF around PSI (DalCorso et al., 2008). In *C. reinhardtii*, the *pgrl1* mutant showed an enhanced H_2 photoproduction (Tolleter et al., 2011; Godaux et al., 2015) while the double mutant *pgrl1 hydg* cannot reactivate photosynthesis under anoxic conditions (Godaux et al., 2015).

A previous genomic survey identified that among the eukaryotes with secondary plastids, the diatom *Thalassiosira*

pseudonana and the excavate *Euglena gracilis* have the most pronounced anaerobic capabilities (Atteia et al., 2013). In anoxic conditions, the excavate *Euglena gracilis* degrades its reserve polysaccharide, paramylon (β-1,3-glucan) (Iwasaki et al., 2019) into myristyl myristate (wax esters) composed of saturated fatty acids and alcohols with chain lengths of 10-18 (Hoffmeister et al., 2005; Inui et al., 2017). During this process, a mitochondrial anaerobic respiration takes place with complex I reducing rhodoquinone that is reoxidized by fumarate reductase (Nakazawa et al., 2018). Unlike common fermentation products described in *C. reinhardtii*, wax esters are accumulated in cells instead of being excreted (Inui et al., 1982; Catalanotti et al., 2013). In addition to wax esters, *E. gracilis* can produce other fermentative metabolites such as lactate and succinate (Tomita et al., 2016). *E. gracilis* also possesses a mitochondrial pyruvate: $NADP^+$ oxidoreductase (PNO), an enzyme close to PFO (Rotte et al., 2001; Nakazawa et al., 2003). In a work in 1963, a hydrogenase activity has also been mentioned in *E. gracilis* without any supporting data though (Hartman and Krasna, 1963).

In some diatoms, it was previously demonstrated that an anaerobic respiration pathway called dissimilatory nitrate reduction to ammonium (DNRA) is active during the first hours under anoxic conditions (Kamp et al., 2011; Catalanotti et al., 2013; Kamp et al., 2013; Kamp et al., 2016). Nitrate accumulated at a high intracellular concentration is reduced into nitrite by Nitrate reductase (NR) in the cytosol and nitrite is reduced in the chloroplast into ammonium by a Nitrite reductase (NIR) using FDX as electron donors. Finally, ammonium is excreted out of the cell rather than being assimilated (Lomas and Glibert, 2000; Kamp et al., 2011; Kamp et al., 2013; Kamp et al., 2015). Based on a genomic data survey in four diatoms (*Thalassiosira pseudonana*, *Phaeodactylum tricornutum*, *Fragilariopsis cylindrus* and *Pseudo-nitzschia*) it was found that only *T. pseudonana* nuclear genome also codes for PFO, PFL and HYDA1 (Atteia et al., 2013).

In *E. gracilis* and *T. pseudonana*, this raises the question of the role of hydrogenase in photosynthetic electron transport under anoxic conditions. In addition, previous studies indicated that CEF around PSI is very low in oxic condition in diatoms (Bailleul et al., 2015) and in *E. gracilis* (Gain et al., 2021). However, the activity of CEF under anoxic conditions has never been studied. Therefore, in this work, we have measured photosystems and hydrogenase activities of *T. pseudonana* and *E. gracilis* in anoxic conditions.

2 Material and methods

2.1 Strains and growth conditions

Axenic strain of *Thalassiosira pseudonana* (CCMP 1335) is a gift from Angela Falciatore and Benjamin Bailleul (IBPC, Paris, France). *T. pseudonana* was grown under low photosynthetic photon flux density (PPFD) of 50 μmol photons.$m^{-2}.s^{-1}$ [white light-emitting diode (LED)], 12 h light – 12 h dark) at 18°C, in artificial sea water (salinity of 33 g.L^{-1}) F/2 liquid medium (Guillard and Ryther, 1962; Guillard, 1975) with silica (Sigma-Aldrich,

G9903). Axenic strain of *Euglena gracilis* (SAG 1224-5/25, obtained from the University of Göttingen; Sammlung von Algenkulturen, Germany), and axenic strain of *Chlamydomonas reinhardtii* (C1' from our collection, derived from 137c strain) were grown under continuous low light (PPFD of 50 µmol photons.m^{-2}.s^{-1}; white LED) at 25°C in Tris-Acetate-Phosphate (TAP) liquid medium (Hutner et al., 1950; Sueoka, 1960; Gorman and Levine, 1965) supplemented with a mix of vitamins (biotin 10^{-7} %, B12 vitamin 10^{-7} % and B1 vitamin 2×10^{-5} %) in the case of *E. gracilis* (Perez et al., 2014), either on solid (1.5% [w/v] agar (Select Agar, Sigma-Aldrich) or in liquid medium. All cultures were performed under air (*i.e.* 21% atmospheric O_2). All experiments were conducted with cells harvested in the middle of the exponential phase of growth. Cell concentration was determined by a Beckman Coulter Z2 Counter Analyser (Z2; Beckman, Indianapolis, IN, USA) with a parameter size around 4 µm (*T. pseudonana*), 8 µm (*C. reinhardtii*) and 15 µm (*E. gracilis*).

2.2 Methods to achieve anoxic conditions

Liquid cultures were centrifuged (4 min at 4,000 *g* for *T. pseudonana* and 10 min at 1,500 *g* for *E. gracilis*) and cell pellets were resuspended in fresh medium (F/2 for *T. pseudonana* and TAP for *E. gracilis*) at 10^7 and 10^6 cells.mL^{-1} for *T. pseudonana* and *E. gracilis*, respectively. Cells were kept in the dark 30 minutes before inducing anoxia. All steps were performed at room temperature (RT, 22 ± 2°C). Erlenmeyer flasks containing cell suspension were transferred in a homemade closed chamber containing less than 0.1 µM of oxygen and bubbled in the dark with nitrogen gas (N_2). Alternatively, cell suspensions were transferred into sealed 4 mL polystyrene cuvettes in presence of glucose (10 mM, Sigma-Aldrich), glucose oxidase (GOX, 2 mg.mL^{-1}, ROTH) and catalase (1000 U.mL^{-1}, Sigma-Aldrich). Depletion in O_2 (time 0) was determined using O_2 sensor spots and optical fibers from Pyroscience (Aachen, Germany). GOX activity produces gluconolactone and H_2O_2 from glucose and O_2 (Bankar et al., 2009). We found that gluconolactone addition in oxic conditions inhibits photosynthetic activity of *T. pseudonana* (Supplementary Figure S1). Therefore, unless specifically specified, the N_2 method was employed to achieve anoxia in this marine diatom. Oxic condition corresponds to aerated cultures (*i.e.* 21% atmospheric O_2).

2.3 Inhibitors preparation

3-(3,4-dichlorophenyl)-1,1-dimethylurea (DCMU), PSII inhibitor, was used at a final concentration of 10 µM. Stock solution of 1 M DCMU was prepared in DMSO. 2-hydroxyacetaldehyde (glycolaldehyde, GA) was used at a final concentration of 20 mM. GA dimer powder was solubilized in water and heated at 65°C for 10 min to obtain 2 M of monomer (Anderson et al., 2007; Roberty et al., 2014). 3-bromopyruvic acid (3BP), was used at a final concentration of 2 mM for *T. pseudonana*

and 10 mM for *E. gracilis*. Stock solution of 1 M 3BP was prepared in water.

2.4 *In vivo* chlorophyll fluorescence measurements

In vivo chl fluorescence measurements were performed on cell suspension, at room temperature (RT, 22 +/- 5°C), with a JTS-10 spectrophotometer (Biologic) with a 640 nm LED source as actinic light. The effective photochemical yield of PSII (ΦPSII) was calculated as ($F_{M'}$ – F_S)/$F_{M'}$ and the maximal quantum yield of PSII (F_V/F_M) was calculated as (F_M – F_0)/F_M , where F_0 is the fluorescence value of dark-acclimated cells, F_S is the fluorescence level in response to a given actinic light, and F_M , $F_{M'}$ are the maximum fluorescence level induced by a 150 ms pulse of saturating light (3,500 µmol photons.m^{-2}.s^{-1}). The relative Electron Transfer Rate (rETR$_{PSII}$, µmol electrons.m^{-2}.s^{-1}) was calculated by multiplying ΦPSII by PPFD used (Genty et al., 1989). All samples were illuminated only once.

2.5 Measurement of P700 oxidation

P700 oxidation was measured on cell suspension in presence of 10% (w/v) ficoll by using a JTS-10 spectrophotometer (Biologic, France) at RT as described in Roberty et al. (2014). The quantum yield of photochemical energy conversion by PSI, was calculated as ($P_{M'}$ – P)/(P_M – P_0) (Klughammer and Schreiber, 2008). P_0 is the absorption level when P700 is fully reduced, P_M is the absorption level when P700 is fully oxidized in the presence of 10 mM DCMU (PSII inhibitor) upon saturating continuous illumination, P_s is the absorbance level under continuous illumination, and $P_{M'}$ is the maximal absorption level reached during a saturating light pulse (3,500 µmol photons.m^{-2}·s^{-1}) on top of the actinic light. The maximal P700 absorbance change was estimated by using the P_M value. The relative Electron Transfer Rate (rETR$_{PSI}$, µmol electrons.m^{-2}.s^{-1}) was calculated by multiplying ΦPSI by PPFD used. All samples were illuminated only once.

2.6 H_2 measurement

H_2 was measured using a hydrogen microsensor (Unisense, UNISENSE A/S, Denmark). The entire set-up was placed in a plastic tent (Glas-Col 108D XX-1H Glove Bag, Templeton Coal Company Inc.) saturated in N_2 to maintain anoxia. *C. reinhardtii*, *T. pseudonana* and *E. gracilis* cell suspensions (10^7, 10^7 and 10^6 cells. mL^{-1}, respectively) were incubated in anoxia during 16 h, and then transferred into a liquid-phase electrode chamber (DW1/AD, Hansatech Instruments) at RT for H_2 measurement. For each measurement and after stabilization of the signal in the dark, the slope (linear) was determined after 1 min of illumination (200 µmol photon.m^{-2}.s^{-1}; RGB LED), during 5 min.

2.7 Phylogeny analysis

We used sequences of PGRL1, PGR5 of *E. gracilis*, *T. pseudonana* and *C. reinhardtii*, and of HYDA1 of *C. reinhardtii* and *T. pseudonana* to retrieve sequences using homology searches by BLAST against sequences of the non-redundant protein sequence database of the NCBI and sequences from other databases (MMETSP and data publicly available). We retrieved the top 2000 sequences with an E-value cut-off lower than $1e^{-10}$ and aligned them using MAFFT with the quick alignment settings (Katoh and Standley, 2013). Block selection was then performed using BMGE (Criscuolo and Gribaldo, 2010) with a block size of 3 for PGR5 and PGRL phylogeny and a block size of 4 for HYDA1 and the BLOSUM30 similarity matrix. We generated preliminary trees using Fasttree (Price et al., 2010) and "dereplication" was applied to robustly supported monophyletic clades using TreeTrimmer (Maruyama et al., 2013) to reduce sequence redundancy. Then a second tree was obtained using MAFFT and BMGE with the same settings, and we used this tree to select manually the final set of sequences. Finally, proteins were realigned with MUSCLE (Edgar, 2004), block selection was carried out using BMGE with the same settings as above, and trees were generated using IQ-TREE with 100 bootstrap repetitions with the LG4X model.

2.8 Statistical analyses

Experiments were performed with at least two independent biological replicates. Comparisons between two treatments were made using two-tailed *t*-tests, comparisons involving more than two treatments were made using a one-way ANOVA and the variation amongst means in relation to treatments was tested by using two-way ANOVA. All statistical analyses were performed using Microsoft Excel software with a threshold of significance at 0.95 ($p < 0.05$).

3 Results

3.1 Distinct chlorophyll fluorescence signatures in anoxic conditions in *E. gracilis* and *T. pseudonana*

We compared chl *a* fluorescence kinetics (3 seconds of illumination at subsaturating light) of *E. gracilis* and *T. pseudonana* cells during dark acclimation under oxic or anoxic conditions. In oxic conditions, no change in fluorescence curves, or significant differences in maximal quantum efficiency of PSII (F_V/F_M) (Figures 1A, B), and relative electron transfer rate of PSII ($rETR_{PSII}$) values could be observed over time in the dark for both species (Figures 1E–H). In *E. gracilis*, F_V/F_M in anoxia is always slightly reduced (Figure 1E) while $rETR_{PSII}$ is decreased by 31% from 2 h of anoxia and up to 86% after 24 h (Figure 1G). After 24 h, this is accompanied by a progressive increase of the fluorescence
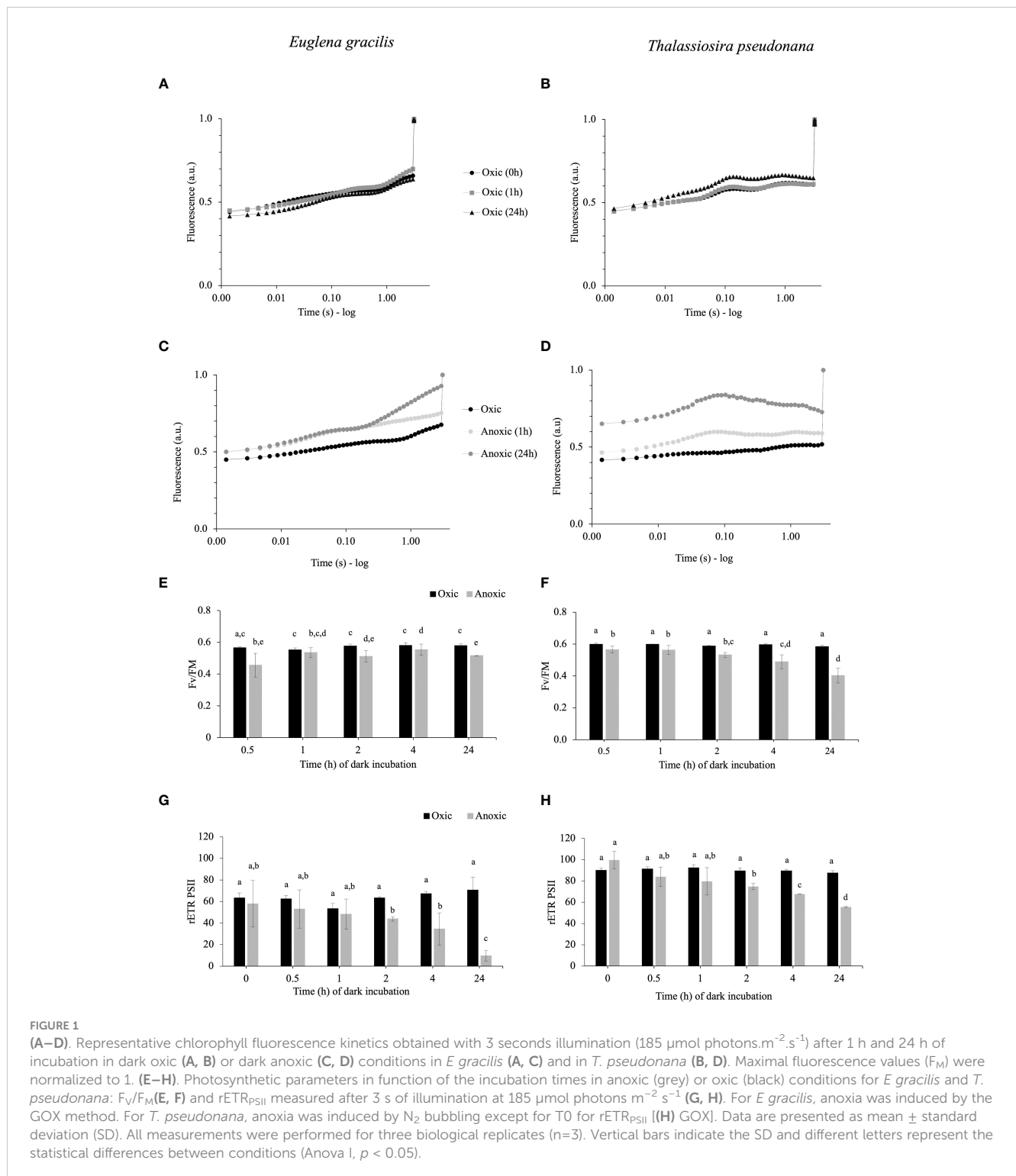
signal during the first seconds of illumination (Figure 1C), indicating a progressive limitation in the availability of electron acceptors. In *T. pseudonana* in anoxic conditions, there is a progressive decrease of F_V/F_M (from 0.6 in control conditions to *ca.* 0.4 after 24 h in anoxia) (Figure 1F). The $rETR_{PSII}$ after 3 s also progressively significantly decreases over time in anoxic conditions (by *ca.* 40% after 24 h) (Figure 1H). After 24 h, this is accompanied by a peculiar signature in the fluorescence curves: in a few ms, the fluorescence signal reaches a maximal transient value which is close to F_M and then it decreases (Figure 1D).

3.2 3-Bromopyruvate impairs PSII activity at the onset of light under anoxic conditions

After dark anoxic incubation, the occurrence of significant $rETR_{PSII}$ after 3 s of illumination in *E. gracilis* (Figures 1C, G) and *T. pseudonana* (Figures 1D, H) reflects the availability of oxidized photosynthetic electron acceptors, and therefore the activity of at least one pathway able to reoxidize photosynthetic electron acceptors in anoxic conditions. To determine if the availability of oxidized photosynthetic electron acceptors during the onset of light depends on a catabolic pathway, we tested the effect of 3-bromopyruvic acid (3BP). 3BP has a large range of possible targets pertaining to the catabolism (Honer Zu Bentrup et al., 1999; Shoshan, 2012; Pedersen, 2012; Sprowl-Tanio et al., 2016). We selected 3BP concentrations (2 mM for *T. pseudonana* and 10 mM for *E. gracilis*) that inhibit after 10 min about 80% of the dark oxygen consumption rate by the mitochondrial respiration in oxic conditions (Supplementary Figure S2). In both species, addition of 3BP under anoxic conditions 10 min before illumination almost fully abolished F_V/F_M and $rETR_{PSII}$ (at least by 80%) while it had a lesser impact on $rETR_{PSII}$ and F_V/F_M in oxic conditions (Figure 2). These results suggest that in both species resuming photosynthetic chain activity is more dependent on catabolism under anoxic conditions than in oxic conditions in both *T. pseudonana* and *E. gracilis*.

3.3 No evidence for a sustained hydrogenase activity in anoxic conditions in *T. pseudonana* and *E. gracilis*

C. reinhardtii $rETR_{PSII}$ at the onset of light under anoxic conditions depends on the activity of an oxygen-sensitive hydrogenase (HYDA1) that oxidizes FDX, the acceptor of PSI (Godaux et al., 2013; Godaux et al., 2015). When turning our attention to hydrogenase phylogeny, no gene coding related to *C. reinhardtii* HYDA1 hydrogenase could be identified in *E. gracilis*. A search performed with the sequences of other hydrogenases (Ni-Fe and Fe-only hydrogenases, *from Hydrogenovibrio marinus* (KDN94743.1) and *C. reinhardtii* (AAR04931.1), respectively) also yielded no result. The only sequence found was a protein closely related to the NAR (nuclear architecture related) protein family

FIGURE 1
(A–D). Representative chlorophyll fluorescence kinetics obtained with 3 seconds illumination (185 µmol photons.m^{-2}.s^{-1}) after 1 h and 24 h of incubation in dark oxic **(A, B)** or dark anoxic **(C, D)** conditions in *E gracilis* **(A, C)** and in *T. pseudonana* **(B, D)**. Maximal fluorescence values (F$_M$) were normalized to 1. **(E–H)**. Photosynthetic parameters in function of the incubation times in anoxic (grey) or oxic (black) conditions for *E. gracilis* and *T. pseudonana*: F$_V$/F$_M$**(E, F)** and rETR$_{PSII}$ measured after 3 s of illumination at 185 µmol photons m^{-2} s^{-1} **(G, H)**. For *E gracilis*, anoxia was induced by the GOX method. For *T. pseudonana*, anoxia was induced by N$_2$ bubbling except for T0 for rETR$_{PSII}$ [**(H)** GOX]. Data are presented as mean $\pm$ standard deviation (SD). All measurements were performed for three biological replicates (n=3). Vertical bars indicate the SD and different letters represent the statistical differences between conditions (Anova I, $p < 0.05$).

(EG_transcript_7200). In contrast, a sequence related to *C. reinhardtii* hydrogenase HYDA1 is found in *T. pseudonana* (B8CGB6_THAPS) and in a limited number of other Coscinodiscophyceae representatives such as *Cyclotella meneghiniana* and *Skeletonema marinoi* while grouping strongly with high bootstraps value (BS=100) with different bacteria (Proteobacteria). We were however unable to retrieve clear, expected, taxonomic groups (Figure 3), questioning vertical

evolution of mechanisms linked to hydrogen. In both *E. gracilis* and *T. pseudonana* cells maintained in anoxic conditions, max H$_2$ evolution rates were around 5 pmol min^{-1} µg chl^{-1} and they did not increase upon subsequent illumination under anoxic conditions. These values were not different from the values measured in dark oxic conditions (Figure 4). In *C. reinhardtii*, used as a control, H$_2$ evolution rate was also very low in dark anoxic or oxic conditions (*ca.* 6 pmol min^{-1} µg chl^{-1}). However, in *C. reinhardtii* in anoxic
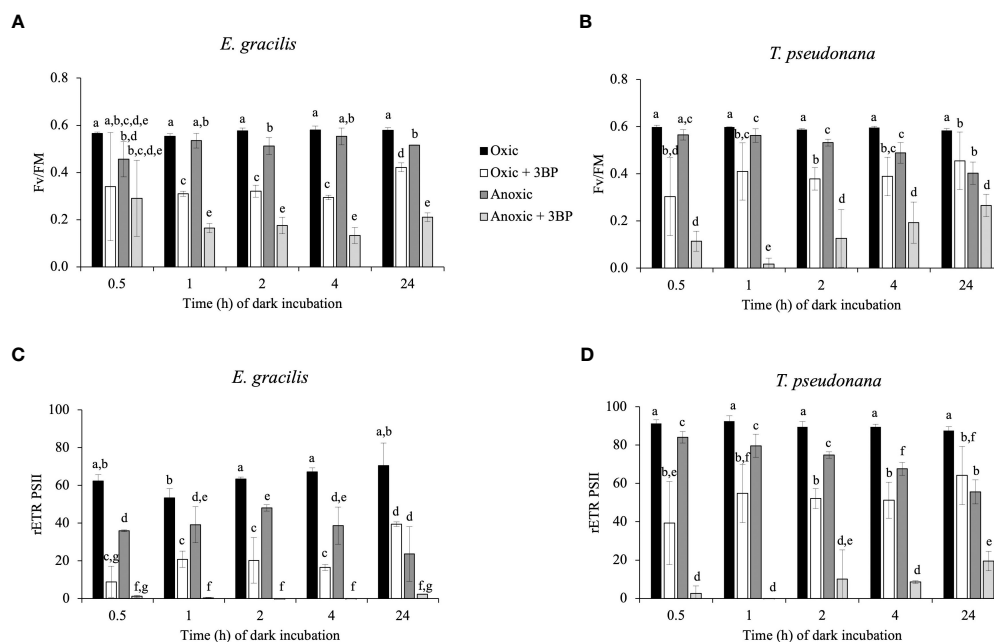
FIGURE 2
Impact of 3-bromopyruvic acid (3BP, 10 mM for *E. gracilis* and 2 mM for *T. pseudonana*) on F_V/F_M **(A, B)**, and rETR$_{PSII}$ (3s illumination at 185 μmol photons.m^{-2}.s^{-1}, **C, D**) in function of dark incubation under oxic (control, black and white) or anoxic (grey) conditions on *E. gracilis* **(A, C)** and *T. pseudonana* **(B, D)**. Data are presented as mean $\pm$ SD. All measurements were performed for three biological replicates (n=3). 3BP (anoxic solution) was added 10 min before illumination. Different letters represent the statistical differences between conditions (Anova II, $p < 0.05$).

conditions, as expected (Godaux et al., 2013), it strongly increased during subsequent illumination, at about 2.5 nmol min^{-1} μg chl^{-1} and almost 90% of this H$_2$ evolution rate in the light was inhibited in the presence of DCMU (Figure 4).

3.4 The increase in PSII activity depends on the reactivation of CBB under anoxic conditions

In parallel to measurement of *in vivo* H$_2$ evolution in continuous light, we monitored rETR$_{PSII}$. In *E. gracilis* and in *T. pseudonana* we observed a progressive increase of rETR$_{PSII}$ which saturates at similar values after several minutes of illumination in both oxic and anoxic conditions (Figure 5). In *E. gracilis*, despite the low initial rETR$_{PSII}$ in anoxia, the kinetics of reactivation are similar to the one in oxic condition (*i.e.* half-maximum rate is achieved after 30-60 s) (Figure 5A). In *T. pseudonana*, there is a short lag (< 30 s) before rETR$_{PSII}$ increases in anoxia (Figure 5B). After 24 h in anoxia, this delay is associated with a slower reactivation compared to the oxic conditions (Figure 5B).

In *C. reinhardtii*, such an increase of rETR$_{PSII}$ is due to the reactivation of the Calvin-Benson-Bassham (CBB) cycle (Cournac et al., 2002; Godaux et al., 2015). To determine if it is also the case for *E. gracilis and T. pseudonana*, we first tested the effect of different concentrations of glycolaldehyde (GA), reported to inhibit the last enzymatic step of the CBB cycle (phosphoribulokinase), on photosynthetic electron transfer capacity in oxic conditions. In *E. gracilis*, despite

phosphoribulokinase is present (Petersen et al., 2006), addition of GA (up to 100 mM) had no effect on photosynthesis in oxic conditions (Supplementary Figure S3A) and was therefore not tested in anoxic conditions. In *T. pseudonana*, the higher is the GA concentration, the higher is the inhibition of photosynthetic activity (Supplementary Figure S3B). On light-acclimated cells in oxic conditions, the addition of GA (20 mM) led to inhibition of 24% of rETR$_{PSII}$ under low light (185 μmol photons.m^{-2}. s^{-1}) and up to 72% of rETR$_{PSII}$ under high light (2840 μmol photons.m^{-2}.s^{-1}) (Supplementary Figure S3C). Addition of 20 mM GA was then added on *T. pseudonana* cells acclimated during 24 h to anoxic conditions in the dark and it fully prevented the increase of rETR$_{PSII}$ during 10 min continuous illumination in anoxic conditions (Figure 6A). GA addition also partly inhibited rETR$_{PSII}$ after 3 s of illumination in oxic conditions, while it had a lesser effect, or no effect on the rETR$_{PSII}$ after 3 s of illumination in anoxic conditions (Figure 6B).

3.5 PSI is more active than PSII at the onset of light in anoxic conditions

In *C. reinhardtii*, the reactivation of the CBB cycle from dark anoxic conditions requires CEF around PSI in addition to hydrogenase activity (Godaux et al., 2015). To determine if CEF around PSI occurs in anoxic conditions in *E. gracilis* and *T. pseudonana*, we compared the values of rETR$_{PSI}$ and rETR$_{PSII}$ in oxic and after 24h of anoxic conditions (Figure 7). After 30 s of illumination, the ratio between rETR$_{PSI}$ and rETR$_{PSII}$ is higher in
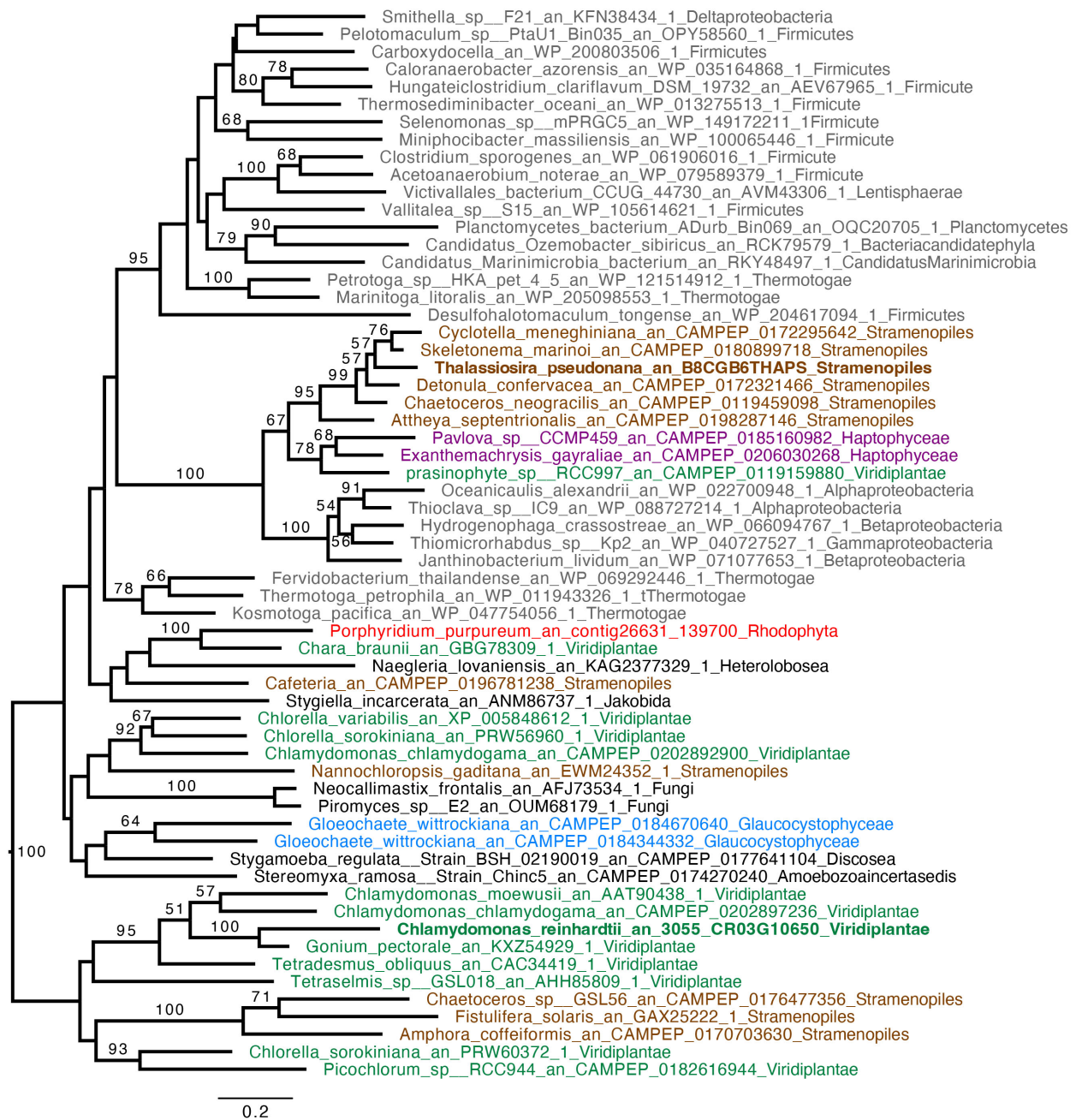
FIGURE 3
Hydrogenase (HYDA1) phylogenetic tree. The tree is midpoint rooted and represents the tree obtained with maximum likelihood approach. We used IQTREE under the LG4X model and performed bootstraps analysis with 100 bootstraps repetition. Bootstrap values > 50% are mapped into the nodes. The scale bar shows the inferred number of amino acid substitutions per site. Sequences are highlighted in grey for Bacteria, in brown for Stramenopila, purple for Haptophyta, light green for Viridiplantae, red for Rhodophyceae, light blue for Glaucophyta while other eukaryotes are in black. Sequences of *C. reinhardtii* and *T. pseudonana* are in bold.

anoxic conditions (3.4 ± 0.1 for *E. gracilis* and 4.9 ± 1.4 for *T. pseudonana*) than in oxic conditions (0.9 ± 0.1 for *E. gracilis* and 1.5 ± 0.1 for *T. pseudonana*). After 5 min of illumination, this ratio significantly decreased in anoxic conditions in both species (1.8 ± 0.1 for *E. gracilis* and 1.5 ± 0.5 for *T. pseudonana*) while it remained stable in control conditions. These values suggest that in both species, CEF around PSI is active in anoxic conditions. In green plants, the main proteins involved in CEF are PGRL1 and PGR5 (DalCorso et al, 2008).

We conducted a phylogenetic analysis to identify putative PGRL1 and PGR5 orthologous genes in *E. gracilis* and in *T. pseudonana*. (Figure 8). The presence of *E. gracilis* (HBDM01013327), *T. pseudonana* (TP04G05420), and *C. reinhardtii* (CR07G05890) indicates a conservation of PGRL1 in those lineages. We also observe in *T. pseudonana* (TP04G06740) an orthologous gene of *C. reinhardtii* PGR5 (CR05G02540) while no clear PGR5 could be retrieved in *E. gracilis*.
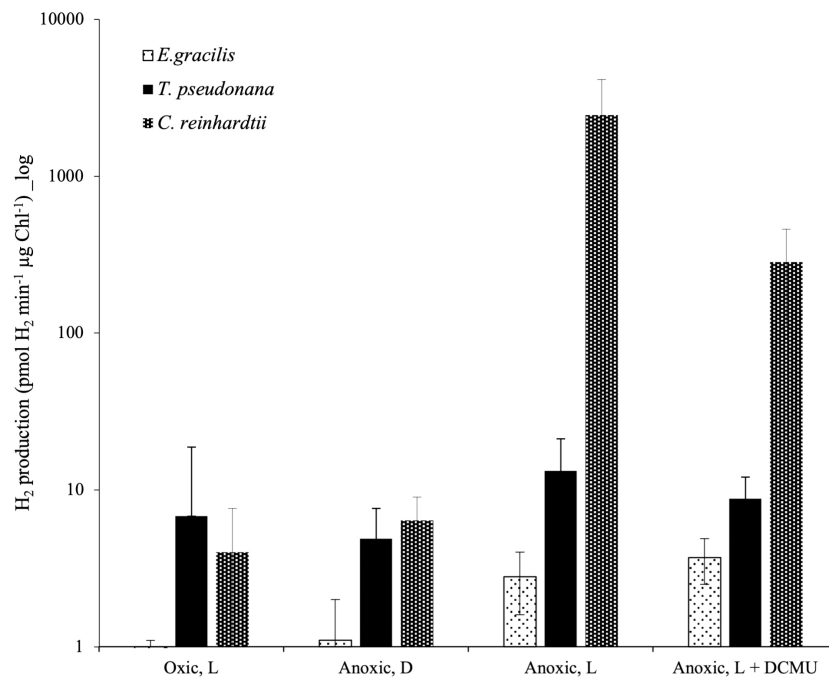
FIGURE 4
In vivo hydrogen evolution rate in *E. gracilis*, *T. pseudonana* and *C. reinhardtii* in oxic and anoxic conditions. Data are presented as mean $\pm$ SD. All measurements were performed on at least three biological replicates. Vertical bars indicate the SD. L, Actinic Light; D, Dark; DCMU was added at 10 μM.

4 Discussion

In their natural environment, some microalgae can be exposed to hypoxic or anoxic environments. In the model green alga *C. reinhardtii*, light-dependent oxygen-sensitive hydrogenase activity, and cyclic electron flow around photosystem I, both contribute to restoring photosynthetic linear electron flow in anoxic conditions (Godaux et al., 2013; Godaux et al., 2015). In this work, we analyzed photosynthetic electron transfer after incubation in dark anoxic conditions in *T. pseudonana* and *E. gracilis*, two model microalgae species that possess canonical fermentative enzymes (Atteia et al.,

2013), but also peculiar fermentative pathways (Nakazawa et al., 2003; Kamp et al., 2011; Kamp et al., 2015; Iwasaki et al., 2019). In both species, PSII activity measured as its relative electron transfer rate (rETR$_{PSII}$) was low at the onset of light after acclimation in the dark under anoxic conditions, but increased progressively (Figure 5), reflecting an increase of photosynthetic LEF. In the primary green alga *C. reinhardtii* increase of LEF in these conditions depends on the reactivation of the CBB cycle (Cournac et al., 2002; Ghysels et al., 2013; Godaux et al., 2015). In green plants, addition of glycolaldehyde (GA), inhibits phosphoribulokinase, an essential enzyme of the CBB cycle, and
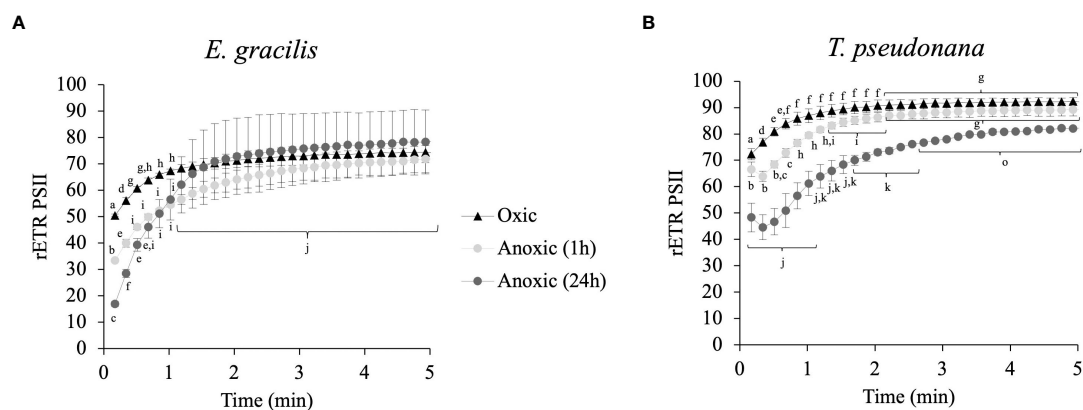

FIGURE 5
Relative electron transfer rate (rETR$_{PSII}$) kinetics during continuous illumination (185 μmol photons.m^{-2}.s^{-1}) for different anoxic incubation times, compared to oxic control (dark adapted for 1 h) in *E gracilis* **(A)** and *T. pseudonana* **(B)**. Data are presented as mean $\pm$ SD; at least two biological replicates. Different letters represent the statistical differences between conditions (Anova I, $p < 0.05$).
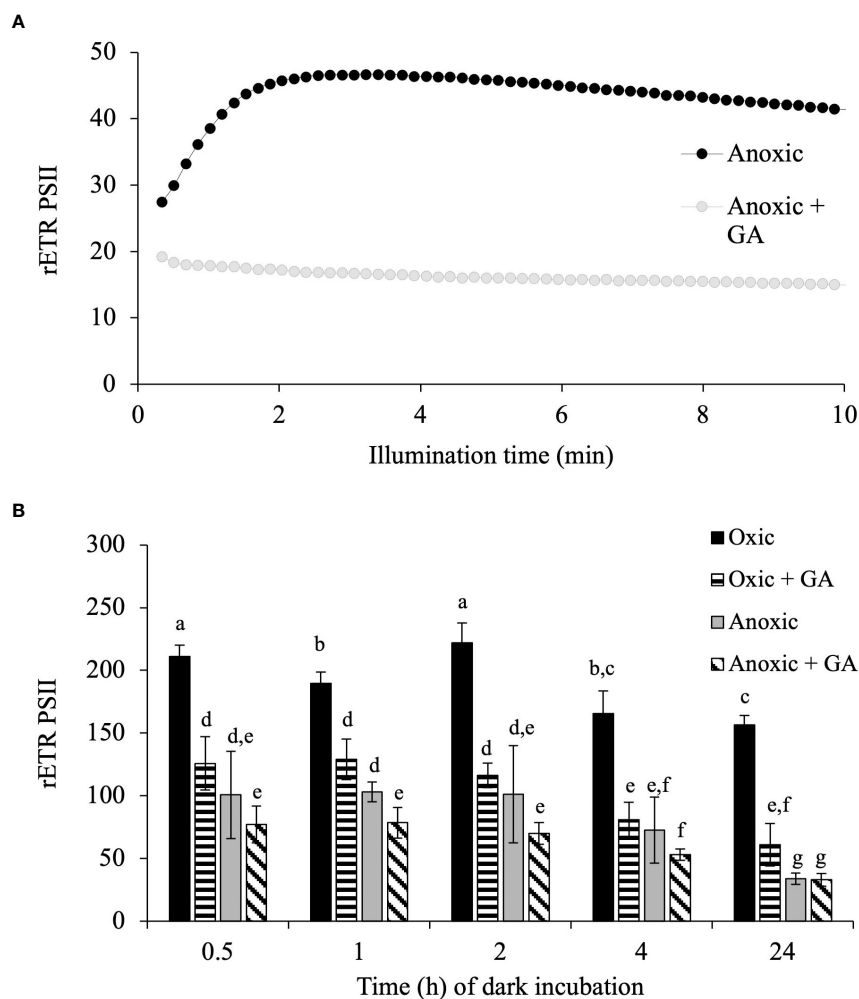
FIGURE 6
Impact of glycolaldehyde in *T. pseudonana*. **(A)** relative Electron Transfer Rate (rETR) of PSII, µmol electron. m^{-2}. s^{-1}) in *T. pseudonana* during continuous illumination (185 µmol photons. m^{-2}. s^{-1}) after 1 h of anoxic incubation. 20 mM glycolaldehyde (+ GA) was added 10 min prior illumination. **(B)** Impact of glycolaldehyde (GA, 20 mM) on rETR$_{PSII}$ (3s illumination at 885 µmol photons.m^{-2}. s^{-1}) in function of incubation time in the dark in oxic (control) or anoxia on *T. pseudonana*. Data are presented as mean $\pm$ SD. All data were performed for three biological replicates. Different letters represent the statistical differences between conditions in function of time of dark incubation (Anova II, $p < 0.05$).

therefore the photosynthetic electron transport rate (Sicher, 1984; Takahashi and Murata, 2005). In *T. pseudonana* after 24h in anoxic conditions, addition of GA prevents the increase of PSII activity upon continuous illumination conditions (Figure 6A). Despite GA may have side effects on other enzymes (see e.g. Jayakody et al., 2011) these results strongly suggests that increase of PSII activity is due to resuming of CBB activity in *T. pseudonana*. Kinetics of activation in both *T. pseudonana* and *E. gracilis* are similar to those observed in *C. reinhardtii* (Takahashi and Murata, 2005; Godaux et al., 2015) and in the cyanobacteria Aphanocapsa (Pelroy et al., 1976). In this respect, the significant inhibitory effect of GA on PSII activity after 3 s of illumination in oxic conditions in *T. pseudonana* (Figure 6B) and the absence of lag in PSII activity increase in oxic conditions in both *T. pseudonana* and *E. gracilis* (Figure 5) reinforces the idea that CBB cycle is activated very fast in these microalgal species. In contrast, the minor effect, or the absence of effect of GA on the initial activity of PSII in anoxia in *T. pseudonana* (3s, Figure 6B) suggest that the initial PSII activity (3s) is independent of the CBB cycle activity in anoxia and therefore relies on another electron sink.

4.1 Cyclic electron flow around PSI is active in anoxia and may contribute to resuming photosynthetic activity

In *C. reinhardtii*, two alternative electron pathways, namely HYDA1, a Fe-Fe hydrogenase that accepts electrons at the acceptor side of PSI, and CEF around PSI, are also required to resume photosynthesis (Godaux et al., 2015). In *E. gracilis* and *T. pseudonana*, rETR$_{PSI}$ is much higher than rETR$_{PSII}$ at onset of light under anoxic conditions (Figure 7). In green plants, including *C. reinhardtii*, this observation is usually interpreted as a large fraction of PSI operating independently of PSII, and therefore contributing to CEF (Godaux et al., 2015; Fan et al., 2016). Our results therefore indicate that CEF around PSI is large but transient under anoxic
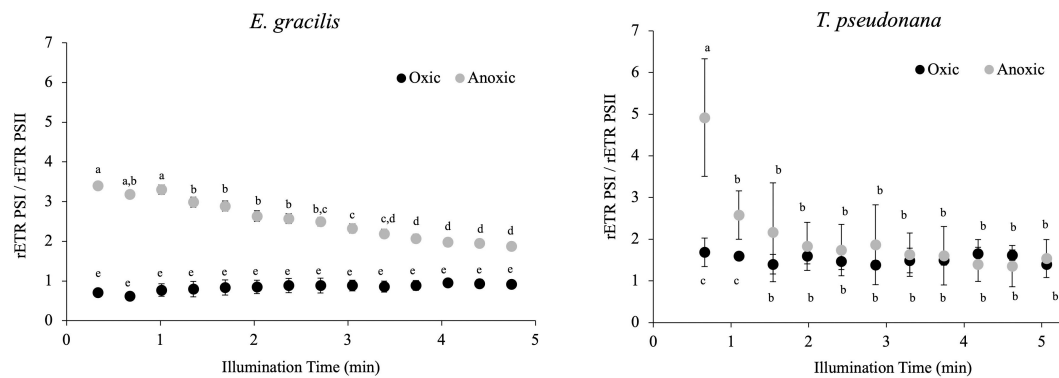
FIGURE 7
Change in the ratio between rETR$_{PSI}$ and rETR$_{PSII}$ during continuous illumination (185 µmol.photons.m^{-2}.s^{-1}) after 24 h in the dark under anoxic or oxic conditions (control) in *E. gracilis* and *T. pseudonana*. Data are presented as mean $\pm$ SD. All measurements were performed for three biological independent culture replicates (n = 3). Different letters represent the statistical differences between conditions (ANOVA I, $p < 0.05$).

conditions, whereas in comparison it could be very weak in oxic conditions in both *T. pseudonana* and *E. gracilis*. This is in line with our previous studies indicating that CEF around PSI is very low in oxic condition in diatoms (Bailleul et al., 2015) and in *E. gracilis* (Gain et al., 2021). CEF is also higher in anoxic conditions than in oxic conditions in *C. reinhardtii* (Alric, 2010), suggesting that the mechanisms behind LEF and CEF partitioning may be broadly shared in photosynthetic eukaryotes. In this respect, the main proteins involved in CEF in green plants, PGRL1 and PGR5 (DalCorso et al, 2008), have orthologs in *T. pseudonana* and at least PGRL1 has an ortholog in *E. gracilis* (Figure 8). In addition, in *E. gracilis* two gene sequences (HBDM01044504, HBDM01072671) are related to PGR proteins (Figure 8).

4.2 Very low hydrogenase activities in *T. pseudonana* and *E. gracilis*

Based on a previous genomic survey, a gene coding for a hydrogenase was identified in *T. pseudonana* (Atteia et al., 2013). It belongs to the same [FeFe] hydrogenase family that is present in green algae such as *C. reinhardtii* (Figure 3). We show here that this enzyme is shared only by Coscinodiscophyceae among diatoms. This points to an independent lateral gene transfer (LGT) between specific diatoms and bacteria, but the direction is unclear (Figure 3). From a functional point of view, this could, in case of LGT from bacteria to diatoms, correlate with special activities or different use in *T. pseudonana* compared to *C. reinhardtii*. In this respect, HYDEF and HYDG, two maturation factors required for HYDA1 maturation in *C. reinhardtii* have not been found in the genome of *T. pseudonana* (Atteia et al., 2013), further supporting the idea that the *T. pseudonana* [FeFe] hydrogenase does not share a common role with *C. reinhardtii* HYDA1. In *E. gracilis*, no HYDA hydrogenase could be identified but only a protein related to the NAR protein family. NAR protein family most probably evolved from an ancestral Fe-hydrogenase and are known to not produce hydrogen (Hackstein, 2015). H$_2$ evolution was barely detectable in both *T. pseudonana* and *E. gracilis*. These values were also not significantly different between oxic and anoxic conditions, and more specifically not stimulated by light in anoxic conditions (Figure 4). The maximal H$_2$

evolution rates *in vivo* measured here for *C. reinhardtii* are in good agreement with previous values measured in subsaturating light (0.25 to 0.58 nmol H$_2$.min^{-1}.µg chl^{-1}) (Tolleter et al., 2011; Clowez et al., 2015; Godaux et al., 2015) or in saturating light (*ca* 2 nmol H$_2$.min^{-1}.µg chl^{-1}) (Meuser et al., 2012; Godaux et al., 2013). Overall, this makes the role of a hydrogenase putative activity in *T. pseudonana* and *E. gracilis* in photosynthetic electron transfer very unlikely. In this respect, *C. reinhardtii*, hydrogenase-deficient mutants impaired in HYDG or HYDEF maturation factors of HYDA1 are however still able to resume photosynthesis provided that CEF around PSI operates (Ghysels et al., 2013; Godaux et al., 2015). In *C. reinhardtii*, several oxidases directly connected to the photosynthetic electron transfer chain (e.g. Flavodiiron protein or Plastidial Terminal Oxidase) have also been described as electron valves for photosynthetic electrons when O$_2$ released by PSII becomes available (Cardol et al., 2010; Godaux et al., 2015; Burlacot et al., 2018). Still, *C. reinhardtii* oxidases do not contribute to the very initial PSII activity at the onset of light (Godaux et al., 2013). Indeed, as in other green algae (Kessler, 1973; Schreiber and Vidaver, 1974), PSII activity during the first seconds of illumination after an anoxic incubation in the dark strictly depends only on *HYDA1* expression (Forestier et al., 2003; Godaux et al., 2013). This strongly suggests that in *T. pseudonana* and *E. gracilis* at least one O$_2$-independant alternative electron sink is also active under anoxic conditions and contributes to the observed LEF at the onset of light (Figure 5).

4.3 Candidate alternative photosynthetic electron sink under anoxic conditions

At variance with *C. reinhardtii* (Godaux et al., 2013; Clowez et al., 2015), a residual rETR$_{PSII}$ under anoxic conditions can be measured as soon as oxygen is depleted (time "0" in Figures 1G, H). This result agrees with previous results obtained in *E. gracilis* and in *P. tricornutum*, another diatom (Shimakawa et al., 2017), and suggests that the electron sink is already present in oxic conditions. In both *T. pseudonana* and *E. gracilis*, the decrease of rETR$_{PSII}$ capacity at light onset over time under anoxic conditions in the dark (Figures 1G, H)
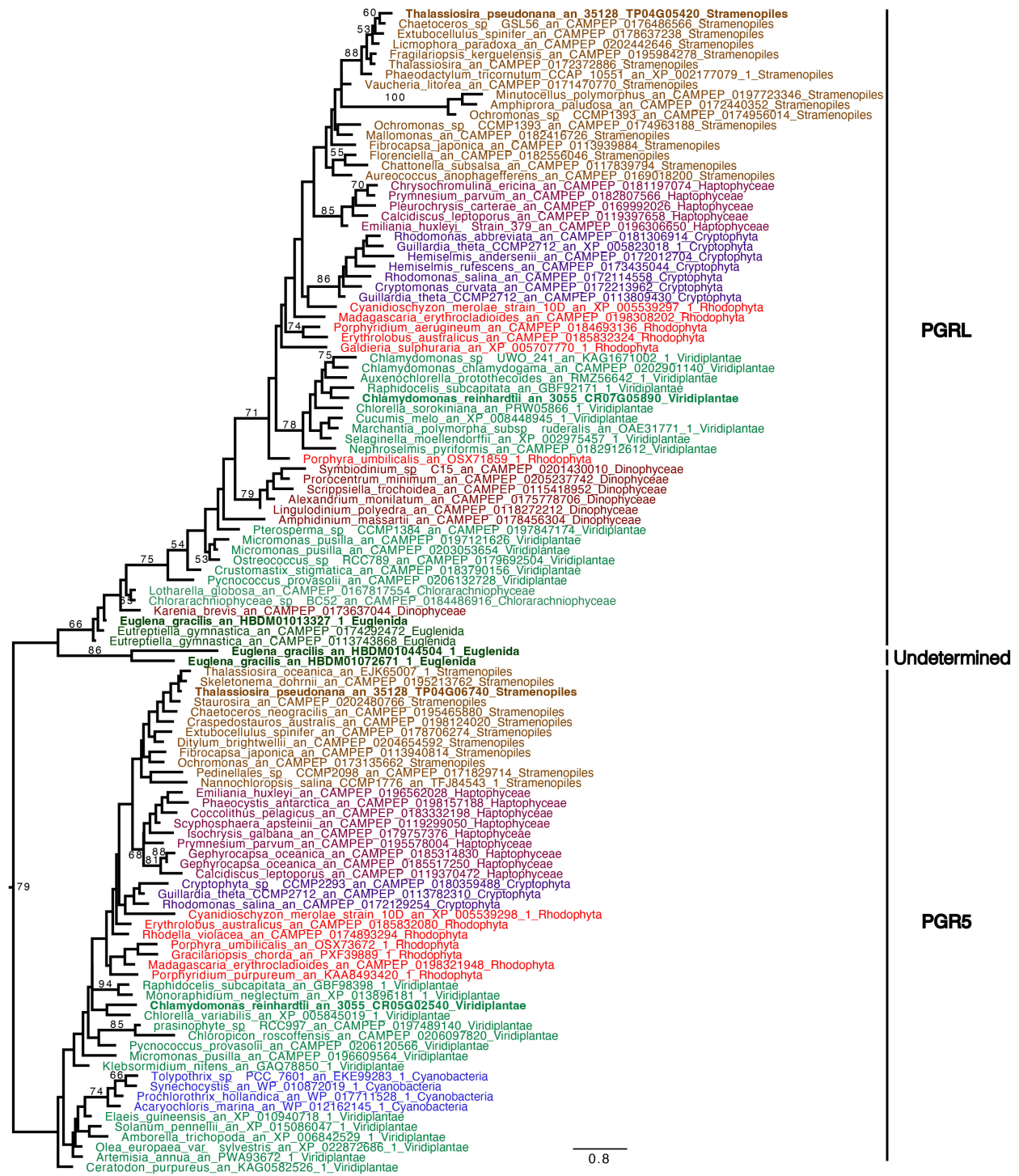
FIGURE 8
Phylogenetic tree of PGR5 and PGRL1. The tree displayed is midpoint rooted and represents the tree obtained with maximum likelihood approach. We used IQTREE under the LG4X model as well as performing bootstraps analysis with 100 bootstraps repetition. Bootstrap values >50% are mapped into the nodes. The scale bar shows the inferred number of amino acid substitutions per site. Sequences are highlighted in blue for Cyanobacteria, in light brown for Stramenopila, and dark brown for Alveolata, purple for Cryptista, garnet for Haptophyta, light green for Viridiplantae, dark green for Euglenozoa and turquoise blue for Chlorarachniophytes, red for Rhodophyceae. Sequences of *C. reinhardtii*, *E. gracilis* and *T. pseudonana* are in bold.

suggests that the capacity of the unknown electron sink(s) decreased. In *T. pseudonana*, this is accompanied by a progressive decrease of Fv/FM (Figures 1D, F), suggesting that the PSII acceptor pool (Q_A, PQ) is more reduced, probably due to an increase of reducing power in the stroma. In addition, PSII activity at light onset is abolished in presence of 3BP to a larger extent in anoxic conditions in both species (Figure 2). 3BP is not a specific inhibitor and may inhibit the glyceraldehyde-3-phosphate dehydrogenase, the hexokinase II, isocitrate lyase, some monocarboxylate transporters and directly or indirectly some respiratory enzymes in other species (Honer Zu Bentrup et al., 1999; Shoshan, 2012; Pedersen, 2012, Sprowl-Tanio et al., 2016). Thus, our results suggest that the capacity of this initial photosynthetic electron sink in anoxic condition may depend on a catabolic pathway, and maybe be related to glycolysis and/or some fermentative pathways.

Under anoxic conditions, *E. gracilis* degrades paramylon, a β-1,3-glucan-type polysaccharide (Barsanti et al., 2001), into wax-ester (Inui et al., 1982; Yamada et al., 2019). This pathway is active when anoxia is reached because wax esters are already detected after 5 min in anoxic conditions (Inui et al., 1982), and it involves a mitochondrial anaerobic respiration (Nakazawa et al., 2018). In anoxic conditions, reducing equivalents are shuttled from cytosol into mitochondria to generate mainly NADPH (Nakazawa et al., 2021). Therefore, in *E. gracilis* we hypothesize that the export of reducing power out of chloroplasts into mitochondria occurs under anoxic conditions and contributes to the observed electron sink at light onset to prevent over-reduction of the photosynthetic apparatus. In *Thalassiosira pseudonana*, nitrate reduction to ammonium by the ferredoxin-NIR (NIR1) activity of the DNRA pathway (Kamp et al., 2011; Kamp et al., 2013) has all the characteristics to correspond to the initial photosynthetic electron sink identified in this work under anoxic conditions, i.e. part of the electrons released at PSII may be used for nitrate reduction during dark/anoxic-to-light transition. Ammonium is excreted out of the cell rather than being assimilated (Lomas and Glibert, 2000; Kamp et al., 2011; Kamp et al., 2013; Kamp et al., 2015). In *Thalassiosira weissflogii* and *Amphora coffeaeformis*, nitrate concentration decreases by half after 2 h and 6 h, respectively, under anoxic conditions (Kamp et al., 2011; Kamp et al., 2013). DNRA is also already active in oxic conditions where this pathway acts as a photosynthetic electron sink to prevent an over-reduction of the photosynthetic apparatus in high light conditions or during an irradiance shift (Lomas and Glibert, 2000; Lomas et al., 2000). In that respect, the rate of NH_4^+ release in *T. weissflogii* in the light reaches 150 fmol NH_4^+ h^{-1} $cell^{-1}$ at 20°C (Lomas et al., 2000), i.e. 0.5 nmol NH_4^+ min^{-1} μg chl^{-1} assuming a chl content of 5 pg per cell (Walter et al., 2015), a value of the same magnitude as the rate of oxygen evolution (ca. 4 nmol O_2 min^{-1} μg chl^{-1}) reported for *T. weissflogii* in oxic conditions (Goldman et al., 2017).

5 Concluding remarks

In conclusion we have observed in *T. pseudonana* and *E. gracilis* that resuming photosynthetic activity under anoxic conditions is possible even in absence of an active hydrogenase. This suggests the presence of anaerobic alternative electron flow with a similar role than *C. reinhardtii* hydrogenase, which helps to prevent an over

reduction of the photosynthetic apparatus and optimizes the CBB reactivation at the onset of light. Further phylogenetic analyses are required to fully understand the diversity and origins of these pathways. In addition, the characterization of the spectrum of fermentation products of these complex algae as well as of photosynthesis regulation under these conditions are still poorly studied compared to other model algae. The study of these organisms may lead to surprising discoveries like original anaerobic pathways (*i.e.* DNRA, wax esters) which can be important for the physiology and the ecology of these algae, but also from a biotechnological point of view with the production of valuable compounds (e.g. wax esters).

Data availability statement

The raw data supporting the conclusions of this article will be made available by the authors, without undue reservation.

Author contributions

PC directed the research. GG, NB, UC, DG and PC designed experiments. GG, TF and NB performed biophysical experiments and physiological analyses. GG, TF, and DG measured hydrogen production. UC performed phylogenetic trees. GG, NB, UC, TF, and PC analyzed and interpreted data. GG, UC, and PC generated all figures and supporting data. GG and PC wrote the manuscript with comments of all authors. All authors contributed to the article and approved the submitted version.

Funding

Acknowledgments

Conflict of interest

The authors declare that the research was conducted in the absence of any commercial or financial relationships that could be construed as a potential conflict of interest.

Publisher's note

All claims expressed in this article are solely those of the authors and do not necessarily represent those of their affiliated

organizations, or those of the publisher, the editors and the reviewers. Any product that may be evaluated in this article, or claim that may be made by its manufacturer, is not guaranteed or endorsed by the publisher.

Supplementary material

The Supplementary Material for this article can be found online at: https://www.frontiersin.org/articles/10.3389/fpls.2023.1186926/full#supplementary-material

References

Alric, J. (2010). Cyclic electron flow around photosystem I in unicellular green algae. *Photosynth Res.* 106, 47–56. doi: 10.1007/s11120-010-9566-4

Anderson, S. E., Wells, J., Fedorowicz, A., Butterworth, L. F., Meade, B., and Munson, A. E. (2007). Evaluation of the contact and respiratory sensitization potential of volatile organic compounds generated by simulated indoor air chemistry. *Toxicological Sci.* 97, 355–363. doi: 10.1093/toxsci/kfm043

Atteia, A., Van Lis, R., Tielens, A. G. M., and Martin, W. F. (2013). Anaerobic energy metabolism in unicellular photosynthetic eukaryotes. *Biochim. Biophys. Acta* 1827 (2), 210–223. doi: 10.1016/j.bbabio.2012.08.002

Bailleul, B., Berne, N., Murik, O., Petroutsos, D., Prihoda, J., Tanaka, A., et al. (2015). Energetic coupling between plastids and mitochondria drives CO_2 assimilation in diatoms. *Nature* 524 (7565), 366–369. doi: 10.1038/nature14599

Bankar, S. B., Bule, M. V., Singhal, R. S., and Ananthanarayan, L. (2009). Glucose oxidase–an overview. *Biotechnol. Adv.* 27 (4), 489–501. doi: 10.1016/j.biotechadv.2009.04.003

Banti, V., Giuntoli, B., Gonzali, S., Loreti, E., Magneschi, L., Novi, G., et al. (2013). Low oxygen response mechanisms in green organisms. *Int. J. Mol. Sci.* 14 (3), 4734–4761. doi: 10.3390/ijms14034734

Barsanti, L., Vismara, R., Passarelli, V., and Gualtieri, P.. (2001). Paramylon (β-1,3-glucan) content in wild type and WZSL mutant of Euglena gracilis. Effects of growth conditions. *J. Appl. Psychol.* 13, 59–65. doi: 10.1023/A:1008105416065

Burlacot, A., Sawyer, A., Cuiné, S., Auroy-Tarrago, P., Blangy, S., Happe, T., et al. (2018). Flavodiiron-mediated O_2 photoreduction links H_2 production with CO_2 fixation during the anaerobic induction of photosynthesis. *Plant Physiol.* 177 (4), 1639–1649. doi: 10.1104/pp.18.00721

Cardol, P., De Paepe, R., Franck, F., Forti, G., and Finazzi, G. (2010). The onset of NPQ and ΔμH⁺ upon illumination of tobacco plants studied through the influence of mitochondrial electron transport. *Biochim. Biophys. Acta*, 1797 (2), 177–188. doi: 10.1016/j.bbabio.2009.10.002

Catalanotti, C., Yang, W., Posewitz, M. C., and Grossman, A. R. (2013). Fermentation metabolism and its evolution in algae. *Front. Plant Sci.* 4, 150. doi: 10.3389/fpls.2013.00150

Clowez, S., Godaux, D., Cardol, P., Wollmann, F.-A., and Rappaport, F. (2015). The involvement of hydrogen-producing and ATP-dependent NADPH-consuming pathways in setting the redox poise in the chloroplast of *Chlamydomonas reinhardtii* in anoxia. *J. Biol. Chem.* 290 (13), 8666–88676. doi: 10.1074/jbc.M114.632588

Cournac, L., Latouche, G., Cerovic, Z., Redding, K., Ravenel, J., and Peltier, G. (2002). *In vivo* interactions between photosynthesis, mitorespiration, and chlororespiration in *Chlamydomonas reinhardtii*. *Plant Physiol.* 129 (4), 1921–1928. doi: 10.1104/pp.001636

Criscuolo, A., and Gribaldo, S. (2010). BMGE (Block mapping and gathering with entropy): a new software for selection of phylogenetic informative regions from multiple sequence alignments. *BMC Evol. Biol.* 10, 210. doi: 10.1186/1471-2148-10-210

DalCorso, G., Pesaresi, P., Masiero, S., Aseeva, E., Schunemann, D., Finazzi, G., et al. (2008). A complex containing PGRL1 and PGR5 is involved in the switch between linear and cyclic electron flow in arabidopsis. *Cell* 132 (2), 273–285. doi: 10.1016/j.cell.2007.12.028

Drew, M. C. (1997). Oxygen deficiency and root metabolism: injury and acclimation under hypoxia and anoxia. *Annu. Rev. Plant Physiol. Plant Mol. Biol.* 48, 223–250. doi: 10.1146/annurev.arplant.48.1.223

Edgar, R. C. (2004). MUSCLE: multiple sequence alignment with high accuracy and high throughput. *Nucleic Acids Res.* 32 (5), 1792–1797. doi: 10.1093/nar/gkh340

Fan, D. Y., Fitzpatrick, D., Oguchi, R., Ma, W., Kou, J., Chow, W. S., et al. (2016). Obstacles in the quantification of the cyclic electron flux around Photosystem I in leaves of C3 plants. *Photosynth. Res.* 129, 239–251. doi: 10.1007/s11120-016-0223-4

Forestier, M., King, P., Zhang, L., Posewitz, M., Schwarzer, S., Happe, T., et al. (2003). Expression of two [Fe]-hydrogenases in *Chlamydomonas reinhardtii* under anaerobic conditions. *Eur. J. Biochem.* 270, 2750e8. doi: 10.1046/j.1432-1033.2003.03656

Gain, G., Vega de Luna, F., Cordoba, J., Perez, E., Degand, H., Morsomme, H., et al. (2021). Trophic state alters the mechanism whereby energetic coupling between photosynthesis and respiration occurs in *Euglena gracilis*. *New Phytol.* 232 (4), 1603–1617. doi: 10.1111/nph.17677

Genty, B., Briantais, J. M., and Baker, N. R. (1989). The relationship between the quantum yield of photosynthetic electron transport and quenching of chlorophyll fluorescence. *Biochim. Biophys. Acta Biomembr.* 990, 87–92. doi: 10.1016/S0304-4165(89)80016-9

Ghysels, B., Godaux, D., Matagne, R.-F., Cardol, P., and Franck, F. (2013). Function of the chloroplast hydrogenase in the microalga *Chlamydomonas*: the role of hydrogenase and state transitions during photosynthetic activation in anaerobiosis. *PloS One* 8, e64161. doi: 10.1371/journal.pone.0064161

Godaux, D., Bailleul, B., Berne, N., and Cardol, P. (2015). Induction of photosynthetic carbon fixation in anoxia relies on hydrogenase activity and proton-gradient regulation-Like1-Mediated cyclic electron flow in *Chlamydomonas reinhardtii*. *Plant Physiol.* 168, 648–658. doi: 10.1104/pp.15.00105

Godaux, D., Emonds-Alt, B., Berne, N., Ghysels, B., Alric, J., Remacle, C., et al. (2013). A novel screening method for hydrogenase-deficient mutants in *Chlamydomonas reinhardtii* based on *in vivo* chlorophyll fluorescence and photosystem II quantum yield. *Int. J. Hydrogen Energy* 38 (2), 1826–1836. doi: 10.1016/j.ijhydene.2012.11.081

Goldman, J., Bender, M., and Morel, F. (2017). The effects of pH and pCO_2 on photosynthesis and respiration in the diatom *Thalassiosira weissflogii*. *Photosynthesis Res.* 132 (1), 83–93. doi: 10.1007/s11120-016-0330-2

Gorman, D., and Levine, R. (1965). Cytochrome f and plastocyanin: their sequence in the photosynthetic electron transport chain of *Chlamydomonas reinhardtii*. *Proc. Natl. Acad. Sci. U. S. A.* 54 (6), 1665–1669. doi: 10.1073/pnas.54.6.1665

Guillard, R. R. L. (1975). "Culture of phytoplankton for feeding marine invertebrates," in *Culture of marine invertebrate animals*. Eds. W. L. Smith and M. H. Chanley (New York, USA: Plenum Press), 26–60.

Guillard, R. R. L., and Ryther, J. H. (1962). Studies on marine planktonic diatoms i. *Cyclotella nana hustedt* and *Detonula confervacea* (Cleve) gran. *Can. J. Microbiol.* 8, 229–239. doi: 10.1139/m62-029

Hackstein, (2015). Eukaryotic fe-hydrogenases – old eukaryotic heritage or adaptive acquisitions? *Biochem. Soc. Trans.* 33 (1), 47–50. doi: 10.1042/BST0330047

Hartman, H., and Krasna, A. I. (1963). Studies on the "Adaptation" of hydrogenase in *Scenedesmus*. *J. Biol. Chem.* 238 (2), 749–757. doi: 10.1016/S0021-9258(18)81331-X

Hemschemeier, A., and Happe, T. (2011). Alternative photosynthetic electron transport pathways during anaerobiosis in the green alga *Chlamydomonas reinhardtii*. *Biochim. Biophys. Acta - Bioenergetics* 1807, 919–926. doi: 10.1016/j.bbabio.2011.02.010

Hoffmeister, M., Piotrowski, M., Nowitzki, U., and Martin, W. (2005). Mitochondrial trans-2-Enoyl-CoA reductase of wax ester fermentation from *Euglena gracilis* defines a new family of enzymes involved in lipid synthesis. *J. Biol. Chem.* 280 (6), 4329–44338. doi: 10.1074/jbc.M411010200

Honer Zu Bentrup, K., Miczak, A., Swenson, D. L., and Russel, D. G. (1999). Characterization of activity and expression of isocitrate lyase in *Mycobacterium avium* and *Mycobacterium tuberculosis*. *J. Bacteriology* 181, 7161–7167. doi: 10.1128/JB.181.23.7161-7167.1999

Hutner, S., Provasoli, L., Schatz, A., and Haskins, C. (1950). Some approaches to the study of the role of metals in the metabolism of microorganisms. *Proc. Am. Philos. Soc.* 94 (2), 152–170.

Inui, H., Ishikawa, T., and Tamoi, M. (2017). Wax ester fermentation and its application for biofuel production. *Adv. Exp. Med. Biol.* 979, 269–283. doi: 10.1007/978-3-319-54910-1_13

Inui, H., Miyatake, K., Nakano, Y., and Kitaoka, S. (1982). Wax ester fermentation in *Euglena gracilis*. *FEBS Lett. EBS.* 150 (1), 89–93. doi: 10.1016/0014-5793(82)81310-0

Iwasaki, K., Kaneko, A., Tanaka, Y., Ishikawa, T., Noothalapati, H., and Yamamoto, T. (2019). Visualizing wax ester fermentation in single *Euglena gracilis* cells by Raman microspectroscopy and multivariate curve resolution analysis. *Biotechnol. Biofuels.* 12 (128), 1–10. doi: 10.1186/s13068-019-1471-2

Jayakody, L. N., Hayashi, N., and Kitagaki, H. (2011). Identification of glycolaldehyde as the key inhibitor of bioethanol fermentation by yeast and genome-wide analysis of its toxicity. *Biotechnol. Lett.* 33, 285–292. doi: 10.1007/s10529-010-0437-z

Kamp, A., de Beer, D., Nitsch, J., Lavik, G., and Stief, P. (2011). Diatoms respire nitrate to survive dark and anoxic conditions. *PNAS.* 108, 5649–5654. doi: 10.1073/pnas.1015744108

Kamp, A., Signe, H., Nils, R.-P., and Peter, S. (2015). Nitrate storage and dissimilatory nitrate reduction by eukaryotic microbes. *Front. Microbiol.* 6, 1492. doi: 10.3389/fmicb.2015.01492

Kamp, A., Stief, P., Bristow, L., Thamdrup, B., and Glud, R. (2016). Intracellular nitrate of marine diatoms as a driver of anaerobic nitrogen cycling in sinking aggregates. *Front. Microbiol.* 7, 1–13. doi: 10.3389/fmicb.2016.01669

Kamp, A., Stief, P., Knappe, J., and de Beer, D. (2013). Response of the ubiquitous pelagic diatom *Thalassiosira weissflogii* to darkness and anoxia. *PloS One* 8, e82605. doi: 10.1371/journal.pone.0082605

Katoh, K., and Standley, D. M. (2013). MAFFT multiple sequence alignment software version 7: improvements in performance and usability. *Mol. Biol. Evol.* 30 (4), 772–780. doi: 10.1093/molbev/mst010

Kessler, E. (1973). Effect of anaerobiosis on photosynthetic reactions and nitrogen metabolism of algae with and without hydrogenase. *Arch. Mikrobiol.* 93 (2), 91-100. doi: 10.1007/BF00424940

Klughammer, C., and Schreiber, U. (2008). Complementary PS II quantum yields calculated from simple fluorescence parameters measured by PAM fluorometry and the saturation pulse method. *PNAS.* 1, 27–35.

Kreuzberg, K. (1984). Starch fermentation *via* a formate producing pathway in *Chlamydomonas reinhardii*, chlorogonium-elongatum and chlorella-fusca. *Physiologia Plantarum* 61 (1), 87–94. doi: 10.1111/j.1399-3054.1984.tb06105.x

Lomas, M., and Glibert, P. (2000). Comparisons of nitrate uptake, storage, and reduction in marine diatoms and flagellates. *J. Phycol.* 36, 903–913. doi: 10.1046/j.1529-8817.2000.99029.x

Lomas, M. W., Rumbley, C. J., and Glibert, P. M. (2000). Ammonium release by nitrogen sufficient diatoms in response to rapid increases in irradiance. *J. Plankton Res.* 22, 2351–2366. doi: 10.1093/plankt/22.12.2351

Maruyama, S., Eveleigh, R. J., and Archibald, J. M. (2013). Treetrimmer: a method for phylogenetic dataset size reduction. *BMC Res. Notes* 6, 145. doi: 10.1186/1756-0500-6-145

Meuser, J. E., D'Adamo, S., Jinkerson, R. E., Mus, F., Yang, W., Ghirardi, M. L., et al. (2012). Genetic disruption of both *Chlamydomonas reinhardtii* [FeFe]-hydrogenases: insight into the role of HYDA2 in H2 production. *Biochem. Biophys. Res. Commun.* 417 (2), 704–709. doi: 10.1016/j.bbrc.2011.12.002

Mus, F., Dubini, A., Seibert, M., Posewitz, M. C., and Grossman, A. R. (2007). Anaerobic acclimation in *Chlamydomonas reinhardtii*: anoxic gene expression, hydrogenase induction, and metabolic pathways. *J. Biol. Chem.* 282 (35), 25475–25486. doi: 10.1074/jbc.M701415200

Nakazawa, M., Ando, H., Nishimoto, A., Ohta, T., Sakamoto, K., Ishikawa, T., et al. (2018). Anaerobic respiration coupled with mitochondrial fatty acid synthesis in wax ester fermentation by *Euglena gracilis*. *FEBS Lett.* 592 (24), 4020–4027. doi: 10.1002/1873-3468.13276

Nakazawa, M., Takahashi, M., Hayashi, R., Matsubara, Y., Kashiyama, Y., Ueda, M., et al. (2021). NADPH-to-NADH conversion by mitochondrial transhydrogenase is indispensable for sustaining anaerobic metabolism in *Euglena gracilis*. *FEBS Lett.* 595 (23), 2922–2930. doi: 10.1002/1873-3468.14221

Nakazawa, M., Takenaka, S., Ueda, M., Inui, H., Nakano, Y., and Miyatake, K. (2003). Pyruvate:NADP$^+$oxidoreductase is stabilized by its cofactor, thiamin pyrophosphate, in mitochondria of *Euglena gracilis*. *Arch. Biochem. Biophys.* 411 (2), 183–188. doi: 10.1016/S0003-9861(02)00749-X

Pedersen, P. L. (2012). 3-bromopyruvate (3BP) a fast acting, promising, powerful, specific, and effective "small molecule" anti-cancer agent taken from labside to bedside: introduction to a special issue. *J. Bioenerg Biomembr.* 44 (1), 1–6. doi: 10.1007/s10863-012-9425-4

Pelroy, R. A., Levine, G. A., and Bassham, J. A. (1976). Kinetics of light-dark CO2 fixation and glucose assimilation by Aphanocapsa 6714. *J. Bacteriol.* 128 (2), 633–643. doi: 10.1128/jb.128.2.633-643.1976

Perez, E., Lapaille, M., Degand, H., Cilibrasi, L., Villavicencio- Queijeiro, A., Morsomme, P., et al. (2014). The mitochondrial respiratory chain of the secondary green alga *Euglena gracilis* shares many additional subunits with parasitic *Trypanosomatidae*. *Mitochondrion* 19 Pt B, 338–349. doi: 10.1016/j.mito.2014.02.001

Petersen, J., Teich, R., Brinkmann, H., and Cerff, R. (2006). A "green" phosphoribulokinase in complex algae with red plastids: evidence for a single secondary endosymbiosis leading to haptophytes, cryptophytes, heterokonts, and dinoflagellates. *J. Mol. Evol.* 62 (2), 143–157. doi: 10.1007/s00239-004-0305-3

Price, M. N., Dehal, P. S., and Arkin, P. A. (2010). FastTree 2 – approximately maximum-likelihood trees for Large alignments. *PloS One* 5 (3), e9490. doi: 10.1371/journal.pone.0009490

Roberty, S., Bailleul, B., Berne, N., Franck, F., and Cardol, P. (2014). PSI mehler reaction is the main alternative photosynthetic electron pathway in symbiodinium sp., symbiotic dinoflagellates of cnidarians. *New Phytol.* 204, 81–91. doi: 10.1111/nph.12903

Rotte, C., Stejskal, F., Zhu, G., Keithly, J. S., and Martin, W. (2001). Pyruvate: NADP+ oxidoreductase from the mitochondrion of *Euglena gracilis* and from the apicomplexan *Cryptosporidium parvum*: a biochemical relic linking pyruvate metabolism in mitochondriate and amitochondriate protists. *Mol. Biol. Evol.* 18 (5), 710–720. doi: 10.1093/oxfordjournals.molbev.a003853

Schreiber, U., and Vidaver, W. (1974). Chlorophyll fluorescence induction in anaerobic *Scenedesmus obliquus*. *Biochim. Biophys. Acta* 368, 97–112. doi: 10.1016/0005-2728(74)90100-5

Shimakawa, G., Matsuda, Y., Nakajima, K., Tamoi, M., Shigeoka, S., and Miyake, C. (2017). Diverse strategies of O2 usage for preventing photo-oxidative damage under CO2 limitation during algal photosynthesis. *Sci. Rep.* 7, 41022. doi: 10.1038/srep41022

Shoshan, M. C. (2012). 3-bromopyruvate: targets and outcomes. *J. Bioenerg. Biomembr.* 44, 7–15. doi: 10.1007/s10863-012-9419-2

Sicher, R. C. (1984). "Glycolaldehyde inhibition of photosynthetic carbon assimilation by isolated chloroplasts and protoplasts," in *Advances in photosynthesis research: proceedings of the VIth international congress on photosynthesis*, vol. 3. (Brussels, Belgium: Springer Netherlands), 413–416).

Sprowl-Tanio, S., Habowski, A. N., Pate, K. T., McQuade, M. M., Wang, K., Edwards, R. A., et al. (2016). Lactate/pyruvate transporter MCT-1 is a direct Wnt target that confers sensitivity to 3-bromopyruvate in colon cancer. *Cancer Metab.* 4, 20. doi: 10.1186/s40170-016-0159-3

Sueoka, N. (1960). Mitotic replication of deoxyribonucleic acid in *Chlamydomonas reinhardi*. *Proc. Natl. Acad. Sci. USA* 46 (1), 83–91. doi: 10.1073/pnas.46.1.83

Takahashi, S., and Murata, N. (2005). Interruption of the Calvin cycle inhibits the repair of Photosystem II from photodamage. *Biochim. Biophys. Acta* 1708 (3), 352–261. doi: 10.1016/j.bbabio.2005.04.003

Tolleter, D., Ghysels, B., Alric, J., Petroutsos, D., Tolstygina, I., Krawietz, D., et al. (2011). Control of hydrogen photoproduction by the proton gradient generated by cyclic electron flow in *Chlamydomonas reinhardtii*. *Plant Cell.* 23 (7), 2619–2630. doi: 10.1105/tpc.111.086876

Tomita, Y., Yoshioka, K., Iijima, H., Nakashima, A., Iwata, O., Suzuki, K., et al. (2016). Succinate and lactate production from *Euglena gracilis* during dark, anaerobic conditions. *Front. Microbiol.* 7, 2050. doi: 10.3389/fmicb.2016.02050

Walter, B., Peters, J., van Beusekom, J. E. E., and St. John, M. (2015). Interactive effects of temperature and light during deep convection: a case study on growth and condition of the diatom *Thalassiosira weissflogii*. *ICES J. Mar. Sci.* 72 (6), 2061–2071. doi: 10.1093/icesjms/fsu218

Yamada, K., Nitta, T., Atsuji, K., Shiroyama, M., Inoue, K., Higuchi, C., et al. (2019). Characterization of sulfur-compound metabolism underlying wax-ester fermentation in *Euglena gracilis*. *Sci. Rep.* 9, 853. doi: 10.1038/s41598-018-36600-z